



Global consumption-based deforestation carbon emissions and regional hotspots: 2001–2020

Dongmei Tang¹, Yuanzhi Yao^{*1}, Rui Li¹, Xia Li^{*1}

¹School of Geographic Sciences, and Key Lab of Geographic Information Science (Ministry of Education), East China Normal University, Shanghai 200241, PR China

Correspondence to: Xia Li (lixia@geo.ecnu.edu.cn); Yuanzhi Yao (zyyao@geo.ecnu.edu.cn)

Abstract. The consumption-based carbon emissions dataset for deforestation provides an important perspective for developing effective emission mitigation policies. However, existing datasets are largely limited to national-scale and lack spatially explicit, high-resolution data at the global level. Here, we present a global, gridded dataset of consumption-based deforestation carbon emissions at 1 km resolution for 2001–2020. The dataset integrates spatial information on road networks, deforestation, and forest carbon fluxes with country-level global trade statistics. Our dataset shows that trade-related deforestation emissions amount to 39.6 Gt CO_{2e}, constituting 31.8% of global deforestation emissions. This new dataset fills a critical gap in spatially explicit consumption-based deforestation emissions data, and supports the development of targeted mitigation strategies from the consumer perspective. It also provides a valuable input for climate and carbon cycle models to assess the contribution of consumption-driven deforestation to global warming. Datasets are available at <https://doi.org/10.6084/m9.figshare.28091879> (Tang et al., 2024).

1 Introduction

Forests represent one of the most important terrestrial carbon sinks and play a critical role in global climate change mitigation due to their high carbon sequestration potential (Cook-Patton et al., 2020). However, global forest cover has continued to decline over recent decades, decreasing from 31.6% of global land area in 1990 to 30.6% in 2015 (Fao, 2015). Although the rate of deforestation has shown a modest decline in recent years, the deforestation continues to occur at an alarming pace. Consequently, deforestation leads to significant carbon emissions, which remained at approximately 1.9 Gt C yr⁻¹ during the period from 2013 to 2022, accounting for about 17% of total anthropogenic emissions (Friedlingstein et al., 2023). Therefore, effectively managing deforestation holds significant potential for mitigating global carbon emissions. International trade remains the primary driver of deforestation, particularly through the expansion of commercial agriculture (Pendrill et al., 2019b; Pendrill et al., 2019a). Large-scale production of commercial agricultural commodities, including livestock, oil palm, rubber, and cash crops, accounts for approximately 40% of tropical deforestation (Wang et al., 2023; Souza Jr, 2023). Previous studies have indicated that 29%-39% of deforestation-related emissions are embodied in international trade (Pendrill et al., 2019b). Although trade promotes global prosperity, it also creates a spatial disconnection



30 between locations of production and final consumption (Wiedmann and Lenzen, 2018). This disconnection complicates
accountability and has led to increasing recognition that mitigating deforestation emissions requires a consumption-based
perspective and policy interventions targeting international supply chains (Pendrill et al., 2019b; Lambin et al., 2018). The
concept of consumption-based deforestation emissions, often referred to as the deforestation emissions footprint, captures the
carbon emissions from deforestation that are attributable to the final consumption of specific countries.

35 Despite its importance, mapping consumption-based deforestation emissions at sub-national or fine spatial scales
remains technically challenging. Most existing studies quantify deforestation footprints at the national level or focus on a
limited number of countries, thereby neglecting substantial spatial heterogeneity within producing regions (Pendrill et al.,
2019b; Pendrill et al., 2019a). This hampers the accurate calculation of trade and consumption footprints, masking and
distorting the causal links between consumers' choices and their environmental impacts, especially in countries with
40 significant spatial variability in carbon storage conditions (Moran et al., 2020). To address this limitation, some studies have
proposed spatially explicit input-output models (SMRIO) that use geospatial data for finer-resolution footprint mapping
(Hoang and Kanemoto, 2021; Kanemoto et al., 2016). However, existing SMRIO applications typically assume proportional
relationships between production and consumption within countries and do not explicitly account for the possibility that
exports originate from specific sub-national regions. As a result, these approaches remain limited in their ability to capture
45 spatial heterogeneity in consumption-driven deforestation emissions and to support geographically targeted mitigation
strategies.

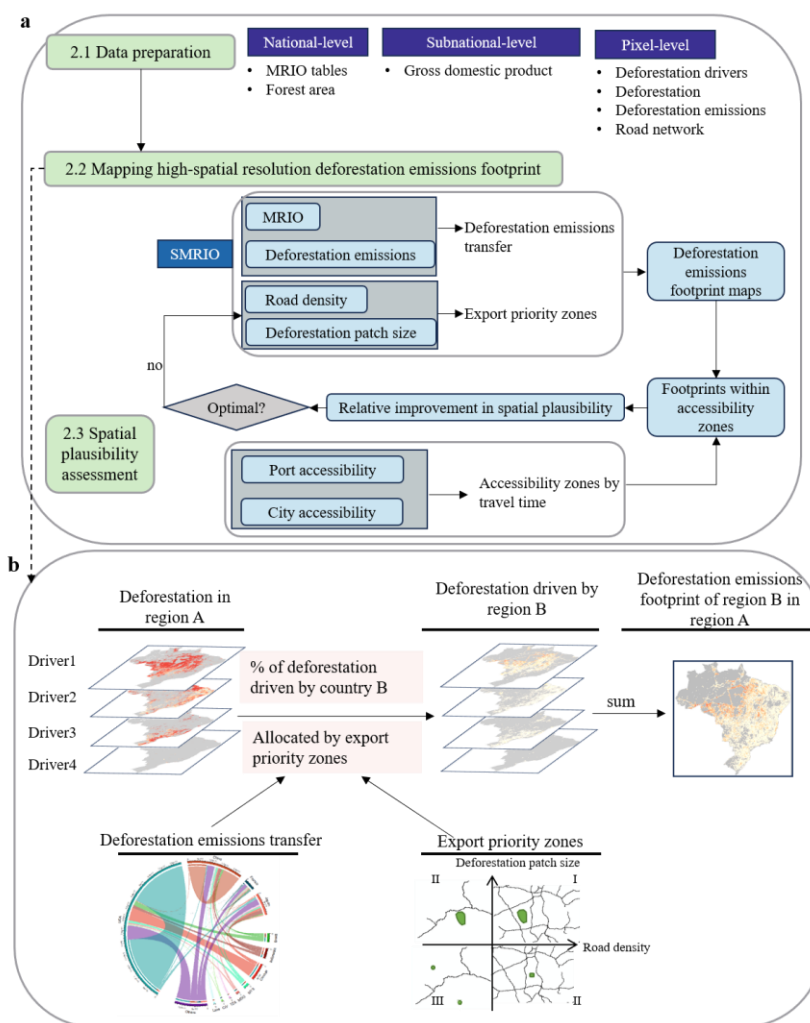
To address these gaps, we developed a global, high-resolution dataset of consumption-based deforestation carbon
emissions by improving existing SMRIO method through pixel-level analysis. By utilizing satellite-based deforestation
observations with economic input-output data, we generate annual global maps of deforestation emissions footprints at a
50 spatial resolution of approximately 1 km for the period 2001–2020. The dataset enables the identification of spatial hotspots
of consumption-driven deforestation and provides a consistent framework for attributing deforestation emissions to final
consumers while retaining the original locations of deforestation. To our knowledge, this is the first global consumption-
based deforestation emissions at the pixel-level. The dataset is intended to support improved accountability for deforestation
emissions, inform supply-chain governance, and facilitate the development of more spatially targeted policies to reduce
55 emissions from deforestation.

2 Data and Methods

In this study, we developed a global, annual, gridded dataset of consumption-based deforestation carbon emissions at a
spatial resolution of approximately 1 km for the period 2001–2020, covering 187 countries and regions. The dataset was
constructed using a spatial multi-regional input–output (SMRIO) framework, which allocates national-level deforestation
60 emission footprints to grid cells based on pixel-level deforestation patch size and road density. The key innovation lies in the



65 plausibility assessment.



70

Figure 1. Overview of the data processing workflow and methodology. (a) Key steps in generating pixel-level deforestation emissions footprint dataset, including data preprocessing, data mapping, and spatial plausibility assessment, together with data sources. Parameter sensitivity analysis was conducted during the data mapping stage using a spatial plausibility assessment approach. (b) Schematic of the SMRIO method. The method integrates pixel-level geospatial data with national-level statistical data, and incorporates export priority zones to enhance the spatial allocation of deforestation emissions at the pixel level.



2.1 Data preparation

2.1.1 Global MRIO tables at the national level

75 MRIO tables provide a comprehensive representation of global production, consumption, and trade flows, and are widely
used to quantify consumption-based environmental footprints (Kanemoto et al., 2016; Lenzen et al., 2018; Liu et al., 2022).
In this study, we utilized a simplified version of the Eora global MRIO tables, specifically the Eora 26, spanning from 2001
to 2020. The Eora 26 tables provide a consistent time series of global MRIO tables with a harmonized 26-sector
classification across 187 countries and regions (Lenzen et al., 2013). These tables allow us to estimate the deforestation
emissions embodied in final demands and the export-oriented share of deforestation for each producing country. These tables
80 form the backbone for calculating national-level consumption-based deforestation emissions.

2.1.2 Pixel-level deforestation, deforestation emissions, and road densities

We obtained annual deforestation data from Hansen et al. (2013), which is derived from time-series analysis of Landsat
images and is updated annually on Global Forest Watch. Deforestation is defined as the complete removal of tree cover
canopy or a stand-replacement disturbance at the scale of Landsat pixels, following Hansen et al. (2013). The deforestation
85 emissions data was obtained from Harris et al. (2021), who also used the annual forest loss data from Hansen et al. (2013),
ensuring consistency with our study's basic data. Harris et al. mapped carbon emissions from global forest extent by
synthesizing information from over 637,000 ground plots, 707,561 waveform lidar observations, and other satellite data into
a spatial forest carbon monitoring framework. To maintain temporal consistency with MRIO tables, we only used
deforestation data up to 2020.

90 Deforestation drivers were classified following Curtis et al. (2018) into five major categories: commodity-driven
deforestation, shifting agriculture, forestry, wildfire, and urbanization. Wildfire-related deforestation was excluded from this
study, as it is not directly linked to economic activities or final consumption. The remaining drivers were mapped to
corresponding economic sectors in the Eora26 classification. Where a single deforestation driver corresponded to multiple
economic sectors, deforestation area was allocated proportionally based on sectoral value added (Hoang and Kanemoto,
95 2021; Kanemoto et al., 2016).

Transportation accessibility was represented using road density, derived from the Global Roads Inventory Project
(GRIP) dataset (Meijer et al., 2018). The GRIP dataset harmonizes approximately 60 geospatial datasets on road
infrastructure and provides a global raster of road density at a 5-arcminute resolution. These pixel-level datasets capture
spatial heterogeneity required to distribute national-level deforestation emissions footprints to 1 km grid cells.



100 2.1.3 Country income classification

Country income categories were obtained from the World Bank and classified into four groups based on gross national income (GNI) per capita: Low income (L), Lower-middle income (LM), Upper-middle income (UM), and High income (H).

2.2 Mapping high-spatial resolution deforestation emissions footprint

2.2.1 Multi-regional input-output model (MRIO)

105 MRIO tables describe the equilibrium of supply and demand among economic sectors across multiple regions, providing detailed information on the flows of goods and services both within and between economies. This balance of supply and demand in MRIO tables can be expressed as Eq. (1):

$$X = T + Y, \quad (1)$$

where $X = [x_i^r]$ denotes total output of sector i in region r ; $T = [z_{ij}^{rs}]$ is the intermediate input-output from sector i in region r to sector j in region s ; $Y = [y_i^{rs}]$ is the final demand in region s supplied by sector i in region r . When the technical coefficient A is introduced, Equation (1) can be reformulated as follows:

$$X = (I - A)^{-1} \times Y, \quad (2)$$

115 where $A = T/X = [a_{ij}^{rs}]$ represents the amount of input of sector i in region r to satisfy the unit value increase in output of sector j in region s ; I is the identity matrix; $(I - A)^{-1} = [b_{ij}^{rs}]$ is the Leontief inverse matrix (L), which represents the gross output from sector i in region r to satisfy one monetary unit of final demand in sector j of region s . To establish a connection between the monetary output and deforestation, we defined a direct deforestation intensity vector f as:

$$f = Q/X, \quad (3)$$

where f is the amount of deforestation per monetary unit of sectoral outputs; $Q = [q_j^s]$ is the deforestation area of sector j in region s , which is also known as deforestation satellite account.

120 Thus, the transfer of deforestation between regions driven by final demand can be calculated by

$$E = \hat{f}Ly, \quad (4)$$

where E is the deforestation transfer matrix; \hat{f} is a diagonal matrix of f ; y is the final demand.

2.2.2. Export priority zones and spatial allocation

To spatially allocate national deforestation emissions footprints to grid cells, we extended the SMRIO framework by introducing export priority zones, which reflect the likelihood that deforestation in a given location is driven by export-oriented production. as follows:



$$F_h^{sr} = \begin{cases} R1_h^r \frac{\sum_i f_i^r \sum_j L_{ij}^{rt} y_j^{ts}}{\sum_i d1_{hi}^r} & \text{if } \sum_j L_{ij}^{rt} y_j^{ts} < \sum_i d1_{hi}^r \\ R1_h^r + R2_h^r \frac{(\sum_i f_i^r \sum_j L_{ij}^{rt} y_j^{ts} - \sum_i d1_{hi}^r)}{\sum_i d2_{hi}^r} & \text{if } \sum_i d1_{hi}^r < \sum_i f_i^r \sum_j L_{ij}^{rt} y_j^{ts} < \sum_i d2_{hi}^r \\ R1_h^r + R2_h^r + R3_h^r \frac{(\sum_i f_i^r \sum_j L_{ij}^{rt} y_j^{ts} - \sum_i d1_{hi}^r - \sum_i d2_{hi}^r)}{\sum_i d3_{hi}^r} & \text{if } \sum_i d2_{hi}^r < \sum_i f_i^r \sum_j L_{ij}^{rt} y_j^{ts} < \sum_i d3_{hi}^r \end{cases}, \quad (5)$$

$$F^s = \sum_{hr} F_h^{sr}. \quad (6)$$

where F^s denotes deforestation emissions footprint map of country s in the world; R denotes map of deforestation emissions for each of $h = 1$ to 4 drivers, and $R1_h^r$, $R2_h^r$, and $R3_h^r$ are maps of deforestation emissions caused by driver h in the first, second and third priority export areas in country r , respectively. d denotes deforestation area, and $d1$, $d2$, and $d3$ are deforestation areas in the first, second and third priority export areas in country r . The embodied deforestation emissions term (fLy) and d are in absolute values; i and j represent the sectors of origin and destination, and r and s denote the countries of production and final sale; t is the country of final demand.

The international demand for export-oriented agricultural products is widely recognized as a significant driver of deforestation (Defries et al., 2010). Profit-driven export trade in agricultural and forestry commodities tends to be concentrated in regions with extensive farmland (Friis and Nielsen, 2019) and well-connected locations (Verburg et al., 2011). Export-oriented agricultural and forestry production tends to occur in regions characterized by large deforestation patches and high transportation accessibility (Meijer et al., 2018). Based on this assumption, export priority zones were identified using two indicators: deforestation patch size and road density. Larger patch sizes and higher road densities were assumed to indicate a higher probability of export-driven deforestation.

Deforestation patches were identified through landscape pattern analysis at a spatial resolution of 30 m, with road density used as a proxy for accessibility. A parameter sensitivity analysis was conducted to determine appropriate thresholds for both indicators. We tested three deforestation patch size (200 × 200, 300 × 300, and 400 × 400 pixels) and seven road density values (50, 60, 70, 80, 90, 100, and 110 m km⁻²). For each parameter combination, a preliminary gridded deforestation emissions footprint dataset was generated and assessed using global accessibility datasets described in Section 2.3. Thresholds were selected based on spatial plausibility criteria. Specifically, the share of deforestation emissions in accessible areas was maximized, while the share allocated to extremely remote regions was minimized. Using these criteria, a deforestation patch size threshold of 300 pixels and a road density threshold of 100 m km⁻² were chosen, resulting in the delineation of three export priority zones (Table 1).

Table 1. the delineation of three export priority in this study

Export priority	Spatial extent
First	$s > 300$ And $d > 100$
second	$(s > 300$ And $d < 100)$ or $(s < 300$ And $d > 100)$



Third	$s < 300$ And $d < 100$
--------------	-------------------------

Notes: s denotes deforested patch size measured in pixels (30×30 m); d denotes the road density (unit: m/km²).

Deforestation emissions embodied in international trade were first allocated to the highest export priority zones. If emissions exceeded the total deforestation emissions of a given zone, the remaining emissions were sequentially allocated to lower export priority zones. In contrast, deforestation emissions driven by domestic consumption were allocated in opposite order, from lower to higher export priority zones.

2.3 Spatial plausibility assessment

2.3.1 Accessibility to cities

Spatial plausibility of the gridded deforestation emissions footprints was assessed based on travel time to cities of different population sizes. We used the global travel time to cities dataset (Weiss et al., 2018), and classified cities into four categories according to population: <10,000; 10,000–20,000; 20,000–50,000; and >50,000 inhabitants. Deforestation emissions footprints located more than five hours from the nearest city were considered less consistent with export-oriented production, as travel times beyond this threshold substantially reduce market access and trade participation (Hochard and Barbier, 2017). Accordingly, travel time to the nearest city was divided into four intervals: <1 h, 1–2 h, 2–5 h, and >5 h.

2.3.2 Accessibility to ports

To further assess spatial plausibility with respect to export-oriented deforestation emissions, travel time to ports was assessed using the Global Accessibility to Ports dataset (Nelson et al., 2019). Ports in the dataset are classified into five categories Large, Medium, Small, Very small, and Any. Deforestation emissions footprints located at very long travel times to ports were considered less closely associated with export-driven deforestation (Gries et al., 2009). Travel time to the nearest port was divided into four intervals for analysis: <24 h, 24–48 h, 48–72 h, and >72 h.

2.3.3 Comparison with conventional spatial allocation approaches

We compared the spatial distribution of deforestation emissions footprints derived from the optimized export priority zones with those obtained using a conventional proportional allocation approach that does not consider accessibility or patch size. The comparison focused on the relative shares of footprints in accessible versus remote areas, illustrating the effectiveness of the proposed approach in enhancing the spatial plausibility of deforestation emissions footprints.



3 Results

3.1 Overview of the global consumption-based deforestation emission footprint between 2001–2020

We estimated global consumption-based deforestation emissions associated with dominant anthropogenic activities for the period 2001–2020 using the improved SMRIO model. During this period, global deforestation resulting in total emissions of 124.5 Gt CO₂e. Notably, 39.6 Gt CO₂e of these emissions were embodied in trade, accounting for 31.8% of total global deforestation emissions. Regionally, the largest consumption-based deforestation emissions were observed in Latin America, Southeast Asia, and the United States (Fig. 2). The deforestation emission footprints in Latin America and the United States remained relatively stable prior to 2015, followed by a marked increase in 2016 and a subsequent decline. This increase was particularly pronounced in Latin America. In Western Europe, Southeast Asia, Sub-Saharan Africa, and China, deforestation emission footprints gradually increased before 2015, peaked around 2016, and then showed a decreasing trend thereafter. In contrast, Russia and the Rest of East Asia exhibited relatively small interannual variability throughout the entire study period.

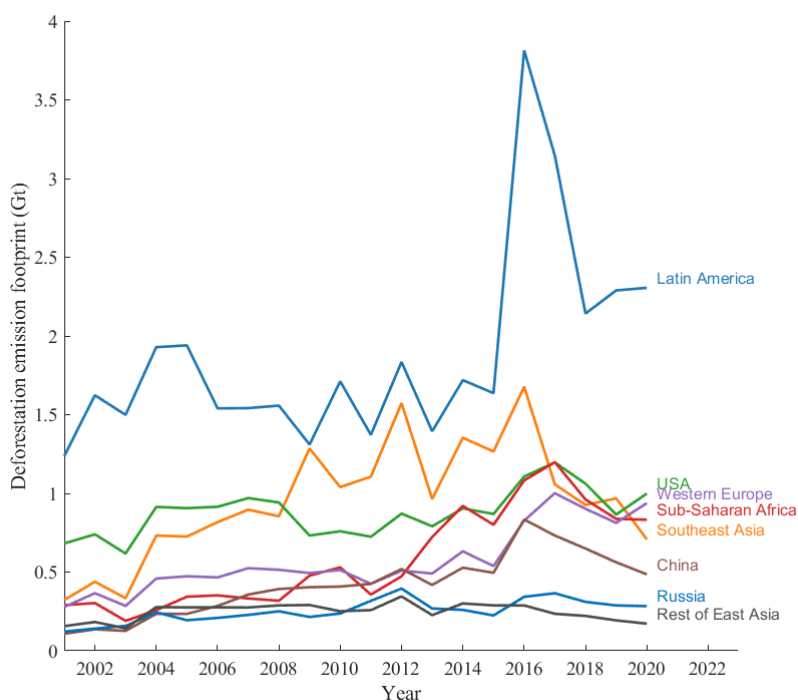
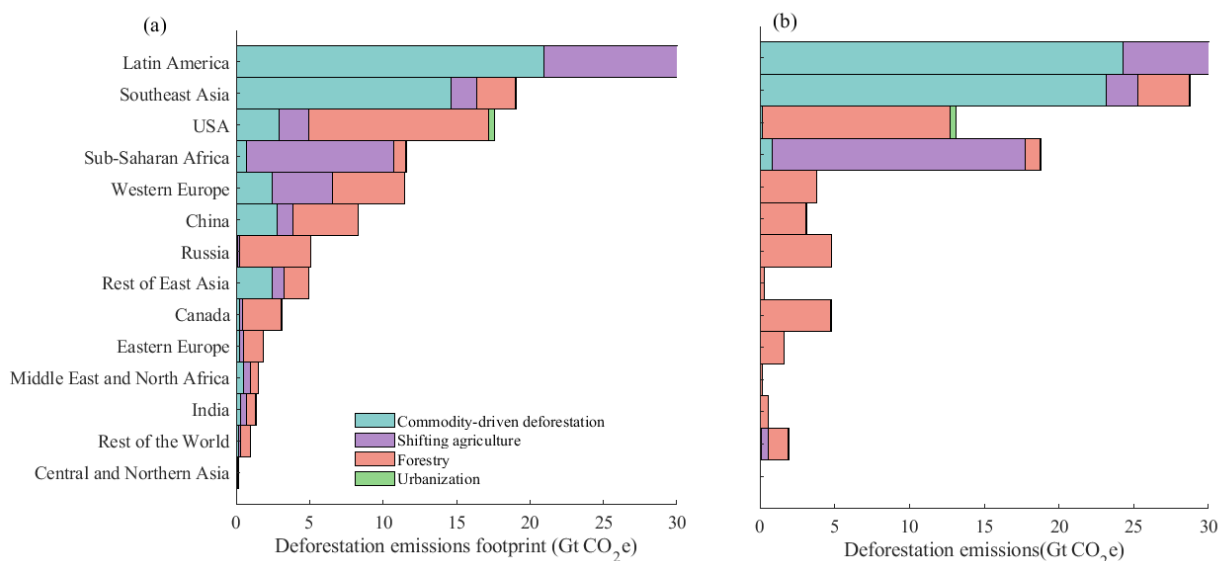


Figure 2. Regional aggregation of global consumption-based deforestation emissions, 2001–2020.

Cumulative deforestation emissions from 2001 to 2020 were further disaggregated by deforestation drivers for both consumption- and production-based perspectives across world regions (Fig. 3). From the consumption perspective, Latin America and Southeast Asia exhibit large emission footprints associated with commodity-driven deforestation. In contrast,



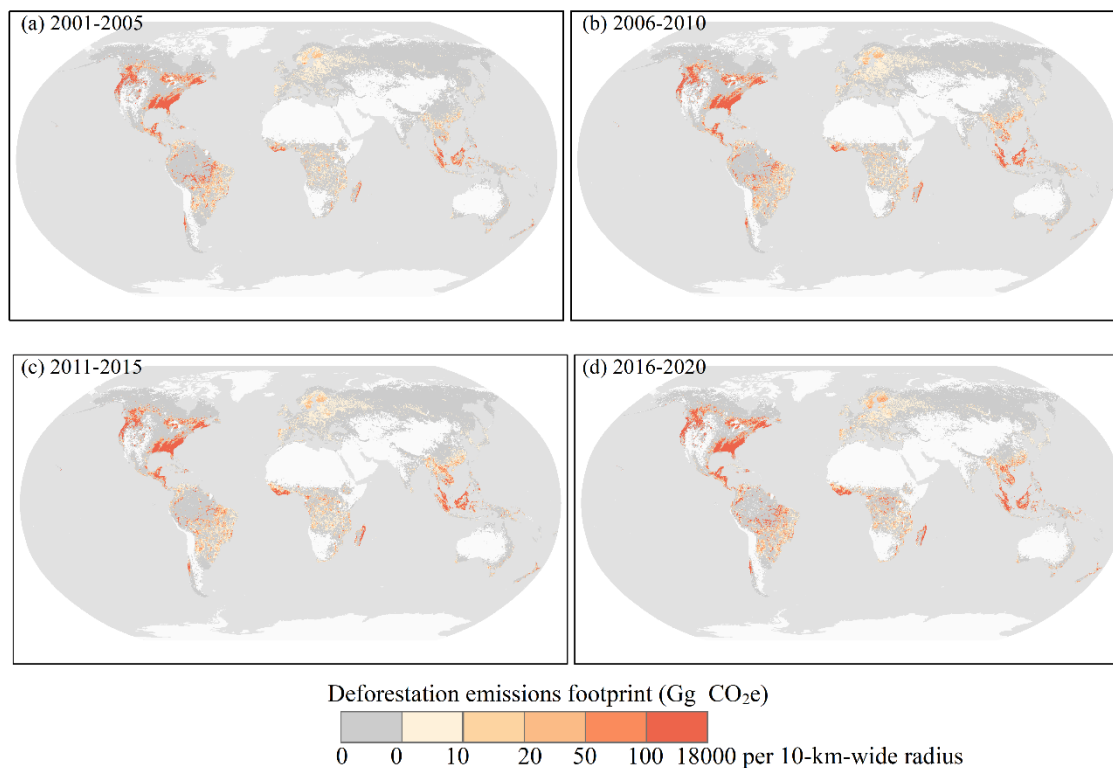
the United States, China, Russia, and Canada show relatively larger contributions from forestry-related activities. Sub-Saharan Africa exhibits the highest share of emissions footprints associated with shifting agriculture (Fig. 3a). From the production perspective, Latin America and Southeast Asia are the dominant contributors to deforestation emissions, with a large proportion of emissions attributable to commodity-driven deforestation. In the United States, Western Europe, China, and other regions, forestry is the primary driver of deforestation emissions, whereas deforestation emissions associated with these regions from a consumption perspective arise from multiple drivers (Fig. 3a, 3b).



200 **Figure 3. Cumulative deforestation emissions by drivers across world regions, 2001–2020: (a) consumption-based deforestation emissions by driver, (b) production-based deforestation emissions by driver.**

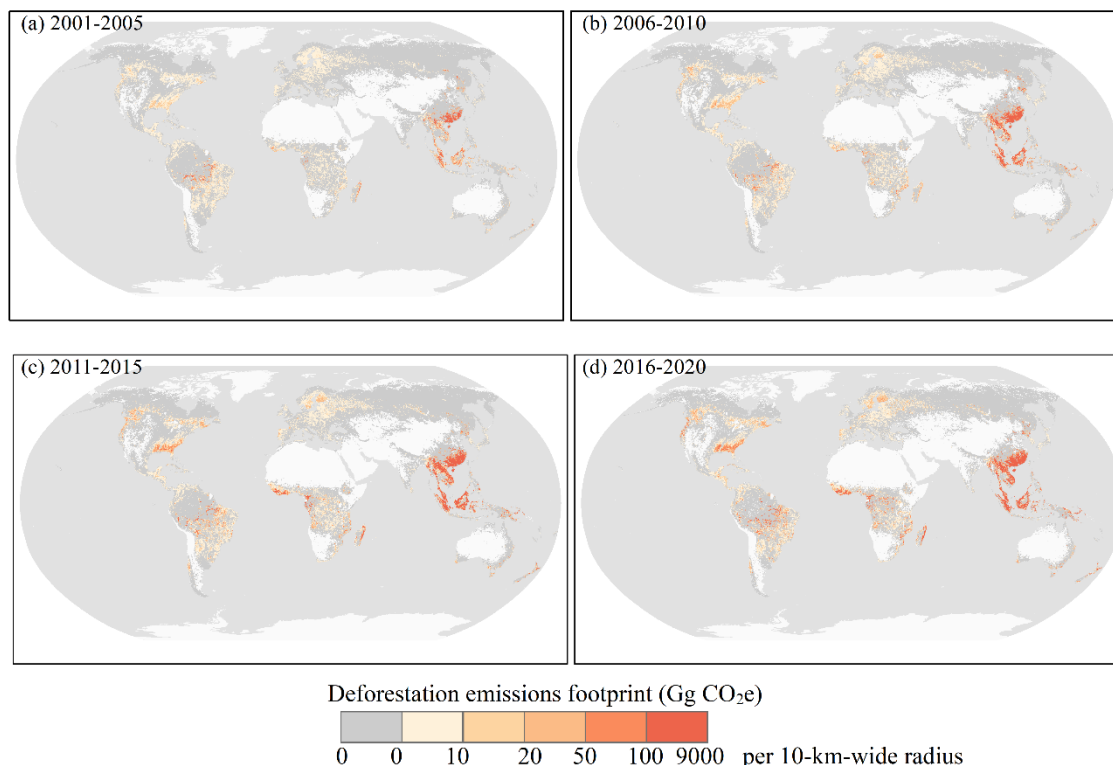
3.2 Spatiotemporal distribution of consumption-based deforestation emissions for major consuming countries

The new dataset, generated using the improved SMRIO model, captures the spatial distribution of consumption-based deforestation emissions at high spatial resolution. Fig. 4 and 5 present four consecutive 5-year cumulative maps of deforestation emission footprints associated with consumption in the United States and China, the two largest net importers of deforestation emissions. Deforestation emissions induced by consumption in the United States are widely distributed across both domestic and international regions. Major emission footprints are observed within the United States and in Southeast Asia, especially in Indonesia and Malaysia. Additionally, hotspots of emissions footprints occur in Brazil, particularly in the Amazon Basin, and in coastal West Africa countries, including Côte d'Ivoire and Liberia, as well as in eastern Madagascar and Chile. Across the four 5-year periods, spatial concentration of deforestation emission footprints increases in Southeast Asia and coastal West African countries after 2005. In South America, deforestation emissions initially decline and then followed by an increase in later periods. In contrast, deforestation emission footprints in other regions show relatively limited temporal variation and remain spatially stable throughout the study period.



215 **Figure 4. Consumption-based deforestation emissions linked to the United States, (a) 2001–2005, (b) 2006–2010, (c) 2011–2015, (d) 2016–2020.**

220 In contrast, China's consumption-based deforestation emissions are more spatially concentrated (Fig. 5). Domestic emission hotspots are mainly located in north China, while international footprints extend primarily to Southeast Asia, particularly Indonesia and Malaysia, as well as to Central and West Africa, including Gabon and Cameroon. Temporally, China's deforestation emission footprint shows a clear expansion after 2005, with increasing spatial intensity and geographic extent in Southeast Asia and African regions during the 2011–2015 and 2016–2020 periods, reflecting a strengthening link between domestic consumption and overseas deforestation. Spatially, China's consumption-driven deforestation emission footprints gradually expand over the first three 5-year periods and remain relatively stable after 2015, with no significant shifts in their spatial distribution.

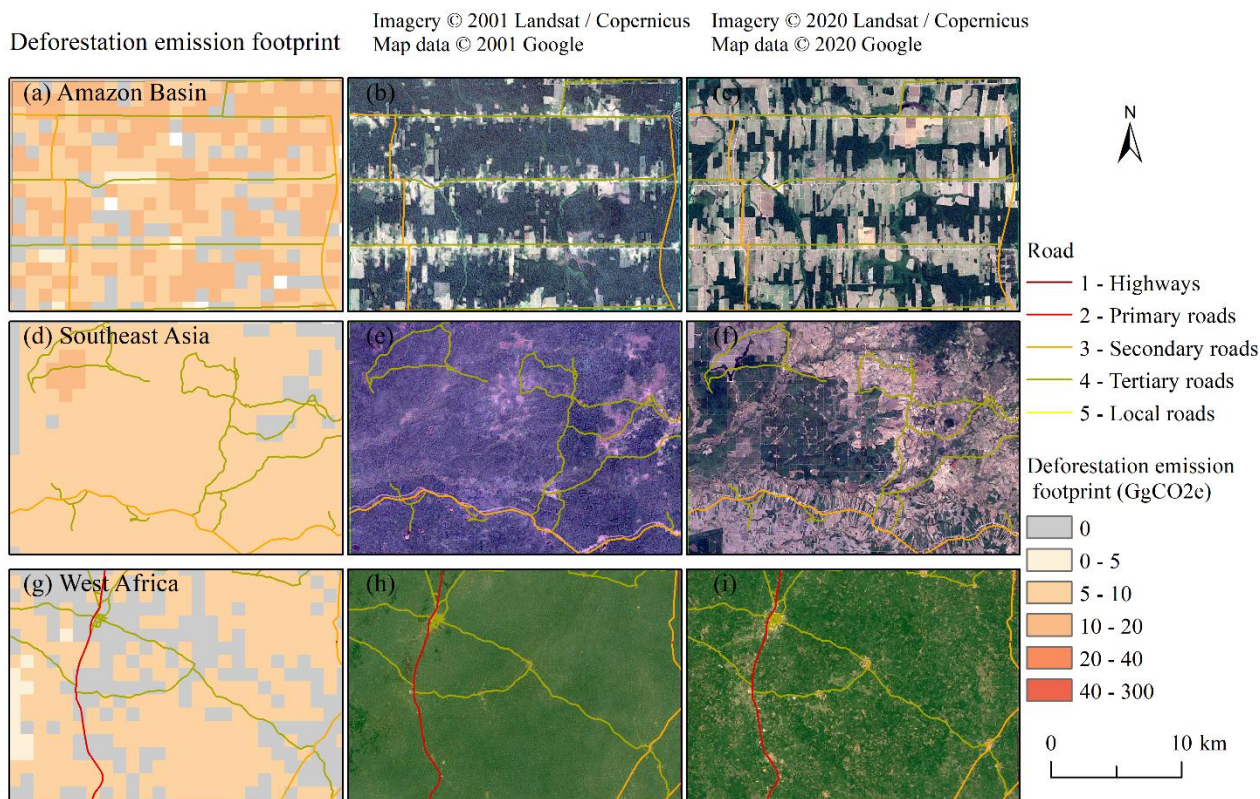


225

Figure 5. Consumption-based deforestation emissions linked to China, (a) 2001–2005, (b) 2006–2010, (c) 2011–2015, (d) 2016–2020.

3.3 Regional examples of consumption-based deforestation emissions

To illustrate the spatial details of the consumption-based deforestation emissions dataset, we selected three sample areas representing hotspots of deforestation emissions footprints, each with a spatial extent of approximately 25 km × 25 km (Fig. 230 6). These samples are located in the Amazon Basin (Brazil), Southeast Asia, and West Africa, representing regions with distinct deforestation drivers, trade linkages, and accessibility conditions. The 1 km resolution allows for clear delineation of the spatial distribution of deforestation emissions footprints associated with different drivers. As shown in the Fig. 6, the deforestation emissions footprints are primarily concentrated in road-dense areas, with relatively larger and more aggregated patch. For instance, in the Amazon Basin, the deforestation emissions footprints extend along roads and gradually spread 235 outward, forming patches with relatively regular shapes (Fig. 6a-6c). In Southeast Asia, where the road network is less evenly distributed than in the Amazon, the deforestation emissions footprints are less aggregated and display a more uniform spatial distribution pattern (Fig. 6d-6f). In the West African region, the road network is less dense than in Southeast Asia, and the deforestation emissions are dispersed into smaller patches, resulting in a more scattered spatial distribution compared with Southeast Asia (Fig. 6g-6i).



240

Figure 6. Regional examples of consumption-based deforestation emissions (Gg CO₂e) at 1 km resolution. Panels (a–c) show cumulative emissions attributable to U.S. final consumption within a 25 km × 25 km sample window in the Amazon Basin from 2001 to 2020, along with high-resolution Google Earth imagery in 2001 and 2020. Panels (d–f) and (g–i) present the corresponding results for the 25 km × 25 km sample windows in Southeast Asia and West Africa. Second column: 2001 imagery; third column: 2020 imagery. Satellite imagery © 2001, 2020 Landsat / Copernicus, Map data © 2001, 2020 Google.

245

3.4 Spatial plausibility assessment using accessibility indicators

The optimal parameter combination used in this study was selected based on the spatial plausibility of the resulting datasets under different parameter settings. Fig. 7 presents the changes in the distribution of global export-driven deforestation emissions across accessibility zones for datasets generated under different parameter combinations, relative to the conventional approach. Compared with the conventional dataset, the dataset produced in this study generally increases the share of deforestation emissions located within areas with travel times to ports of less than 12 hours, while reducing the share in areas with travel times between 12 and 48 hours. Except for parameter combination 2 ($d_{100-S300}$), all other combinations increase the share of deforestation emissions in regions with travel times to ports exceeding 72 hours (Fig. 7a). Similarly, relative to the conventional dataset, the dataset generated in this study increases the share of deforestation emissions in areas with travel times to cities of less than 2 hours, while reducing the share in areas where travel time to cities exceeds 2 hours. The magnitude of change follows a clear gradient: the closer to cities (higher accessibility), the larger the

250

255



increase, whereas more remote areas (lower accessibility) experience larger reductions (Fig. 7b). Considering both port and city accessibility, parameter combination 2 ($d_{100-s_{300}}$) was selected as the optimal setting. Although the increase in emissions within 12 hours of ports under combination 2 ($d_{100-s_{300}}$) is smaller than that under combination 4 ($d_{50-s_{300}}$), it is the only combination that reduces emissions in areas with travel times to ports exceeding 72 hours. In addition, combination 2 ($d_{100-s_{300}}$) achieves the strongest improvement in areas within 1 hour of cities. Based on these considerations, parameter combination 2 ($d_{100-s_{300}}$) was adopted in this study.

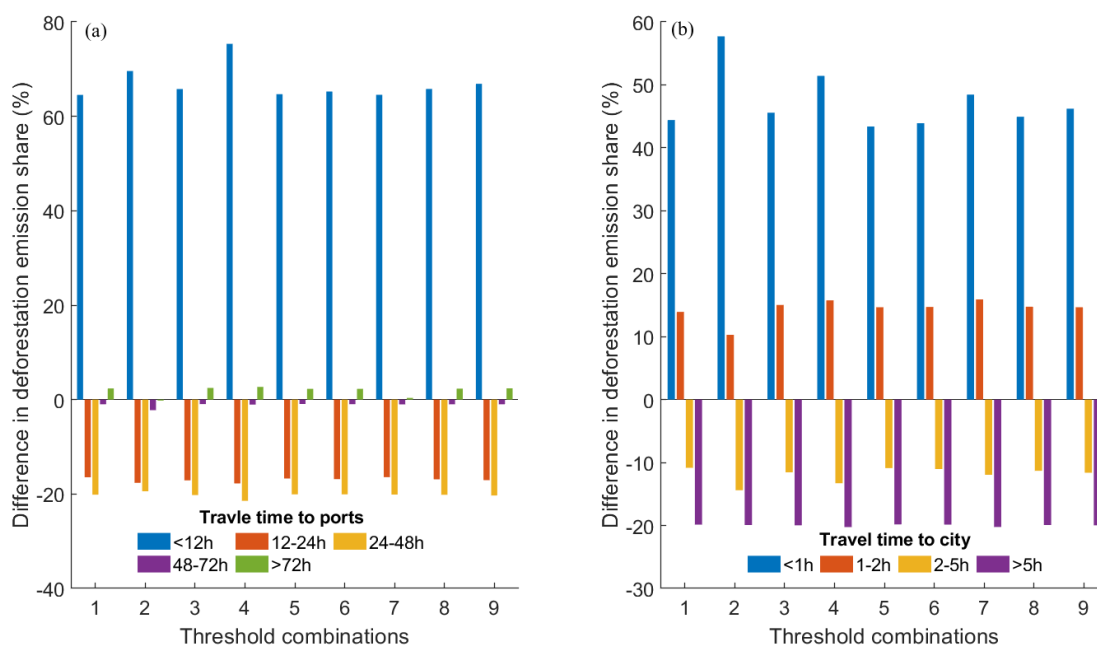
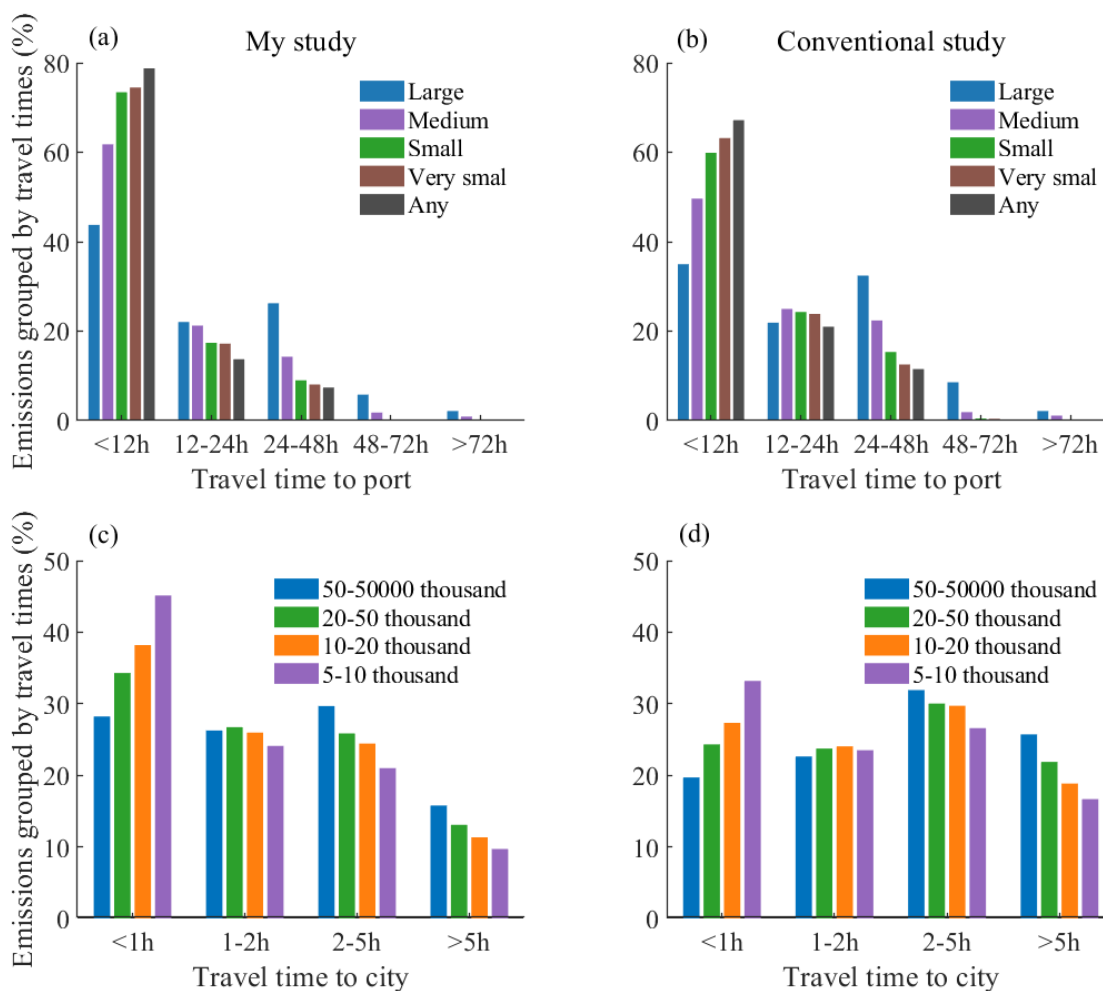


Figure 7. Sensitivity analysis of parameter combinations showing changes in export-driven deforestation emissions across port (a) and city (b) accessibility zones relative to the conventional approach. Nine parameter combinations ($d_{100-s_{400}}$, $d_{100-s_{300}}$, $d_{100-s_{200}}$, $d_{50-s_{300}}$, $d_{60-s_{300}}$, $d_{70-s_{300}}$, $d_{80-s_{300}}$, $d_{90-s_{300}}$, and $d_{110-s_{300}}$) were evaluated, where d denotes road density (m/km^2) and s denotes deforested patch size (pixels, $30 \times 30 \text{ m}$ resolution).

The spatial plausibility of the gridded deforestation emission footprint developed in this study was assessed using an independent global accessibility dataset. Results show that consumption-driven deforestation emissions are concentrated in areas with high accessibility. The proportion of deforestation emissions increases as accessibility improves. Only a minimal fraction of emissions occurs in very remote regions (Fig. 8a and 8c). Compared with conventional approaches, the dataset produced in this study increases the proportion of deforestation emissions in well-accessible areas (e.g., travel time to ports <12 h or to cities <2 h) while reducing the share in less accessible areas (e.g., travel time to ports >12 h or to cities >2 h), with the reductions becoming more pronounced as accessibility decreases.

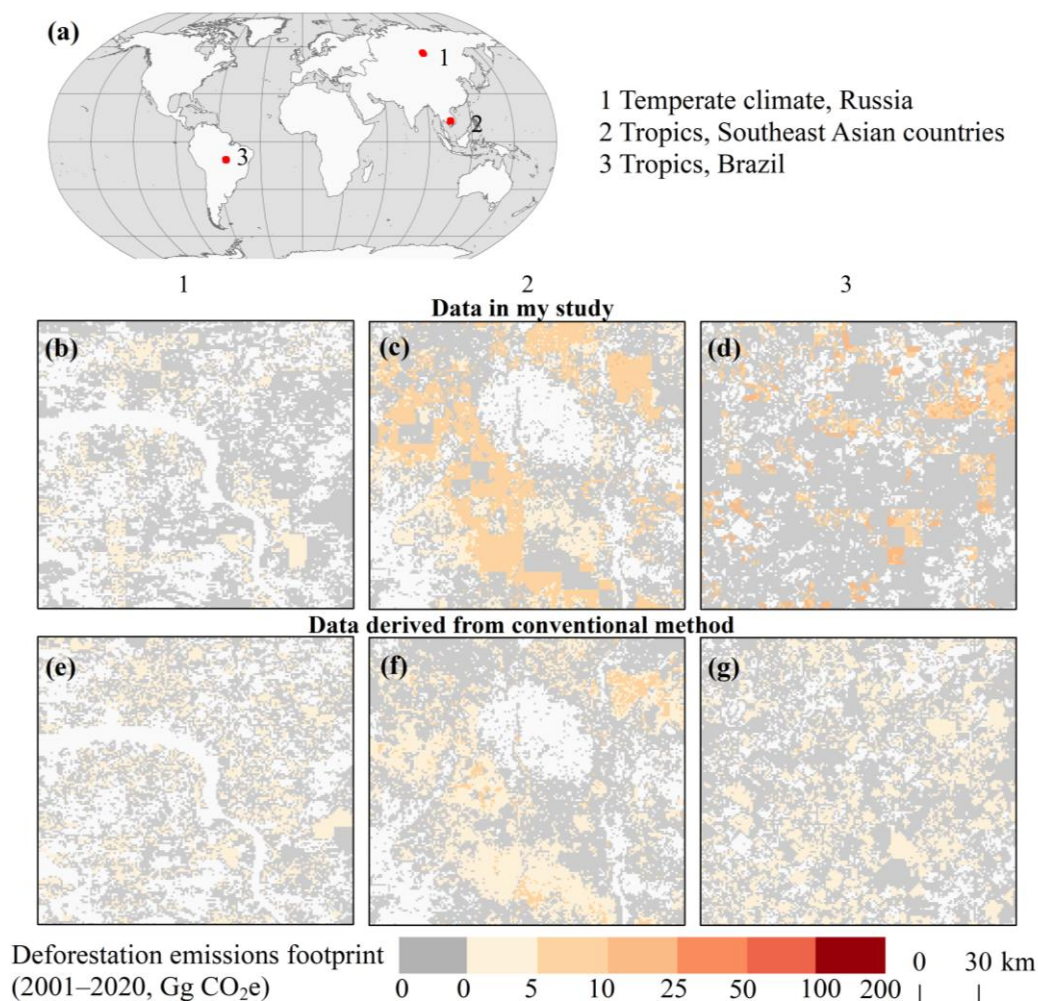


275

Figure 8. Proportion of export-driven deforestation emissions across accessibility zones. Accessibility is measured as travel time to ports (panel a–b) and cities of different population sizes (panel c–d). Panels (a) and (c): this study; panels (b) and (d): conventional methods.

We further compared the spatial distribution patterns of deforestation emission footprints derived from this study with those obtained using the conventional approach (Fig. 9). Using the U.S. consumption-driven deforestation emission footprints as an example, three representative regions with substantial deforestation emissions were selected: Russia (b, e), Southeast Asia (c, f), and Brazil (d, g). These regions span different climate zones and exhibit varying levels of transportation infrastructure. The spatial patterns of deforestation emission footprints in these regions show consistent characteristics. Compared with the conventional approach, the deforestation emissions estimated in this study are confined to a smaller spatial extent and exhibit a more clustered distribution, whereas those derived from the conventional approach are more broadly distributed and relatively uniform across deforested areas. Regional differences are also evident: deforestation emission footprints in Southeast Asia and Brazil are more spatially clustered than those in Russia.

285



290 **Figure 9. Spatial distribution of deforestation emission footprint hotspots from 2001–2020 derived from this study and from the conventional method.**

4 Discussions

4.1 Significance of mapping deforestation emissions embodied in international trade

Deforestation emissions are a significant source of greenhouse gases, making large-scale and accurate accounting crucial for mitigating these emissions. However, at this stage, fine-scale consumption-based inventories of deforestation emissions remain limited. In this study, we utilized an improved SMRIO model to map the global 1 km deforestation emission footprint for 2001–2020 from a consumption-based perspective. During this period, total deforestation emissions amounted to 124.5 Gt CO₂e. Of these emissions, 39.6 Gt CO₂e were embodied in international trade, accounting for 31.8% of global

295



deforestation emissions. The share is slightly higher than that reported for land-use emissions (27%; Hong et al. (2022)) and is comparable to the share of fossil-fuel emissions embedded in international trade (23-30%; Wiedmann and Lenzen (2018)).

300 Land-use and fossil-fuel emissions embedded in international trade have received increasing attention in climate mitigation (Hong et al., 2022; Yang et al., 2020; Wiedmann and Lenzen, 2018; Kanemoto et al., 2016). Our results suggest that deforestation emissions hidden in international trade should also receive similar attention. Accurate accounting of consumption-based deforestation is therefore essential for international climate mitigation initiatives such as REDD+ (Pendrill et al., 2019b; Lambin et al., 2018). The gridded dataset developed in this study provides spatially explicit

305 information that complements national-scale accounting approaches. For example, in West Africa, the dataset captures fine-scale spatial heterogeneity in deforestation emissions footprints associated with cocoa-producing regions in Côte d'Ivoire and Ghana. The gridded representation reveals localized hotspots that are not evident in nationally aggregated statistics, underscoring the value of high-resolution spatial data for informing targeted local policy interventions.

4.2 Comparisons with existing datasets

310 To date, several datasets of deforestation footprint have been developed in previous studies (Pendrill et al., 2019b; Henders et al., 2015). However, these datasets have significant limitations. For instance, some studies focus only on tropical forests (Henders et al., 2015), while others use accounting methods that do not fully capture detailed deforestation emissions (Pendrill et al., 2019b). In addition, many existing datasets are compiled at national scales, which limits their ability to represent spatial heterogeneity in deforestation emissions. Global deforestation footprint datasets derived from SMRIO

315 model partially address the scale limitation. However, these datasets typically distribute footprints uniformly across producing regions, ignoring intra-country spatial heterogeneity (Hoang and Kanemoto, 2021; Yang et al., 2020). In this study, our data overcame these limitations by introducing export priority areas to spatially allocate deforestation emissions, thereby improving the spatial representation of deforestation emission footprints. By integrating spatially explicit deforestation emissions data from Harris et al. (2021), which are consistent with the annual forest loss data from Hansen et al.

320 (2013), our dataset provides a more detailed representation of the spatial distribution of deforestation emissions and enables more precise estimation of deforestation emission footprints.

4.3 Limitations and uncertainties

Although this study provides a global fine-scale dataset of deforestation emission footprints for 2001–2020, several uncertainties should be considered when using the dataset. First, due to the lack of detailed supply-chain information, it is

325 not possible to identify the exact export destinations of deforestation emissions at the sub-national level (Yang et al., 2020). Consequently, this study assumes equal export probabilities across regions, consistent with previous research (Yang et al., 2020). Second, this dataset includes only deforestation emissions associated with economic activities. Emissions from wildfire are excluded because they cannot be directly linked to economic drivers. Third, the temporal coverage of the dataset



330 is constrained by the availability of input–output databases. Input-output tables typically involve significant time lags in
compilation and release (He et al., 2022). In contrast, many underlying datasets used in this study, such as satellite-based
deforestation observations and related drivers, are updated more frequently (Hosseiny et al., 2024; Liu et al., 2025). Once
updated input-output databases become available, our dataset can be readily extended to include more recent years. Future
improvements would benefit from more traceable and transparent global supply-chain data, which would enable more
accurate spatial allocation of consumption-based deforestation emissions.

335 **4.4 Potential applications**

This dataset provides the 1 km gridded deforestation emission footprints associated with the major consuming countries for
the period 2001–2020. Compared with existing datasets, it offers a longer time series, broader spatial coverage, and higher
spatial resolution, enabling detailed analyses of spatial heterogeneity of deforestation emission footprints within countries.
The spatial plausibility of the dataset has been evaluated using accessibility data, demonstrating its suitability for quantitative
340 analyses. The dataset has significant applications in climate change mitigation research from a consumer perspective,
providing essential information for accounting consumption-based deforestation carbon emissions. It is also critical for
designing targeted emission reduction policies in deforestation hotspot regions. In addition, the dataset can serve as input to
climate and carbon cycle models to assess the contribution of consumption-driven deforestation emissions to global warming
and to quantify the relative contributions of major consuming countries to cumulative CO₂ emissions and associated
345 temperature responses.

5 Data availability

The global gridded dataset of consumption-based deforestation carbon emissions for 2001–2020 generated in this study is
publicly available at <https://doi.org/10.6084/m9.figshare.28091879> (Tang et al., 2024). The dataset includes annual global
deforestation emission footprints associated with seven major consuming countries, along with accompanying
350 documentation describing the dataset overview, usage notes, and limitations. The documentation is provided in a
README.txt file. The dataset is provided in GeoTIFF format at a spatial resolution of 30 arc-seconds (approximately 1 km
at the equator). Each grid cell reports annual deforestation-related carbon emissions attributed to the final consumption of
specific countries.

6 Conclusions

355 The proportion of consumption-driven deforestation emissions is comparable to that of consumption-driven fossil fuel
emissions, underscoring the importance of accounting for and mitigating these emissions. Despite their significance, detailed
global datasets on consumption-based deforestation emissions remain scarce. This study presents the first time-series,



gridded datasets of consumption-based deforestation emissions from 2001 to 2020. The dataset indicates that deforestation emissions footprint is increasing in most regions worldwide. Although the use of spatially explicit data addresses some limitations of previous datasets, uncertainties remain, particularly in the allocation of exports from individual regions. Future improvements will require more detailed and traceable supply chain information to enhance the accuracy of consumption-based deforestation emission datasets.

Author contribution

Dongmei Tang: Conceptualization, Methodology, Software, Formal analysis, Visualization, Writing - Original Draft.
365 **Yuanzhi Yao:** Conceptualization, Writing - Review & Editing, Funding acquisition. **Rui Li:** Resources, Writing - Review & Editing, **Xia Li:** Conceptualization, Writing - Review & Editing, Supervision, Funding acquisition.

Competing interests

One of the authors of this manuscript, Yuanzhi Yao, is a member of the editorial board of the journal.

Acknowledgements

370 This study was supported by the Key National Natural Science Foundation of China (Grant No. 42130107), the National Natural Science Foundation of China (Grant No. 42371410) and the National Natural Science Foundation of China for Young Scientists Fund Program C (Grant No. 42501514).

References

- Cook-Patton, S. C., Leavitt, S. M., Gibbs, D., Harris, N. L., Lister, K., Anderson-Teixeira, K. J., Briggs, R. D., Chazdon, R. L., Crowther, T. W., Ellis, P. W., Griscom, H. P., Herrmann, V., Holl, K. D., Houghton, R. A., Larrosa, C., Lomax, G., Lucas, R., Madsen, P., Malhi, Y., Paquette, A., Parker, J. D., Paul, K., Routh, D., Roxburgh, S., Saatchi, S., van den Hoogen, J., Walker, W. S., Wheeler, C. E., Wood, S. A., Xu, L., and Griscom, B. W.: Mapping carbon accumulation potential from global natural forest regrowth, *Nature*, 585, 545-550, 10.1038/s41586-020-2686-x, 2020.
- 380 Curtis, P. G., Slay, C. M., Harris, N. L., Tyukavina, A., and Hansen, M. C.: Classifying drivers of global forest loss, *Science*, 361, 1108-1111, 10.1126/science.aau3445, 2018.
- DeFries, R. S., Rudel, T., Uriarte, M., and Hansen, M.: Deforestation driven by urban population growth and agricultural trade in the twenty-first century, *Nat. Geosci.*, 3, 178-181, 10.1038/ngeo756, 2010.
- FAO: Global forest resources assessment 2015: how are the world's forests changing? , FAO, Rome, 2015.
- 385 Friedlingstein, P., O'Sullivan, M., Jones, M. W., Andrew, R. M., Bakker, D. C. E., Hauck, J., Landschützer, P., Le Quéré, C., Luijkx, I. T., Peters, G. P., Peters, W., Pongratz, J., Schwingshackl, C., Sitch, S., Canadell, J. G., Ciais, P., Jackson, R. B., Alin, S. R., Anthoni, P., Barbero, L., Bates, N. R., Becker, M., Bellouin, N., Decharme, B., Bopp, L., Brasika, I. B. M., Cadule, P., Chamberlain, M. A., Chandra, N., Chau, T.-T.-T., Chevallier, F., Chini, L. P., Cronin, M., Dou, X., Enyo, K., Evans, W., Falk, S., Feely, R. A., Feng, L., Ford, D. J., Gasser, T., Ghattas, J., Gkritzalis, T., Grassi, G., Gregor, L., Gruber,



- 390 N., Gürses, Ö., Harris, I., Hefner, M., Heinke, J., Houghton, R. A., Hurtt, G. C., Iida, Y., Ilyina, T., Jacobson, A. R., Jain, A.,
Jarníková, T., Jersild, A., Jiang, F., Jin, Z., Joos, F., Kato, E., Keeling, R. F., Kennedy, D., Klein Goldewijk, K., Knauer, J.,
Korsbakken, J. I., Körtzinger, A., Lan, X., Lefèvre, N., Li, H., Liu, J., Liu, Z., Ma, L., Marland, G., Mayot, N., McGuire, P.
C., McKinley, G. A., Meyer, G., Morgan, E. J., Munro, D. R., Nakaoka, S.-I., Niwa, Y., O'Brien, K. M., Olsen, A., Omar, A.
M., Ono, T., Paulsen, M., Pierrot, D., Pockock, K., Poulter, B., Powis, C. M., Rehder, G., Resplandy, L., Robertson, E.,
Rödenbeck, C., Rosan, T. M., Schwinger, J., Séférian, R., Smallman, T. L., Smith, S. M., Sospedra-Alfonso, R., Sun, Q.,
395 Sutton, A. J., Sweeney, C., Takao, S., Tans, P. P., Tian, H., Tilbrook, B., Tsujino, H., Tubiello, F., van der Werf, G. R., van
Ooijen, E., Wanninkhof, R., Watanabe, M., Wimart-Rousseau, C., Yang, D., Yang, X., Yuan, W., Yue, X., Zaehle, S., Zeng, J.,
and Zheng, B.: Global Carbon Budget 2023, *Earth Syst. Sci. Data*, 15, 5301-5369, 10.5194/essd-15-5301-2023, 2023.
- Friis, C. and Nielsen, J. Ø.: *Telecoupling: Exploring land-use change in a globalised world*, Palgrave Studies in Natural
Resource Management, Springer, Switzerland 2019.
- 400 Gries, T., Naudé, W., and Matthee, M.: The optimal distance to port for exporting firms, *J. Reg. Sci.*, 49, 513-528, 2009.
- Hansen, M. C., Potapov, P. V., Moore, R., Hancher, M., Turubanova, S. A., Tyukavina, A., Thau, D., Stehman, S. V., Goetz,
S. J., Loveland, T. R., Kommareddy, A., Egorov, A., Chini, L., Justice, C. O., and Townshend, J. R.: High-resolution global
maps of 21st-century forest cover change, *Science*, 342, 850-853, 10.1126/science.1244693, 2013.
- Harris, N. L., Gibbs, D. A., Baccini, A., Birdsey, R. A., de Bruin, S., Farina, M., Fatoyinbo, L., Hansen, M. C., Herold, M.,
405 Houghton, R. A., Potapov, P. V., Suarez, D. R., Roman-Cuesta, R. M., Saatchi, S. S., Slay, C. M., Turubanova, S. A., and
Tyukavina, A.: Global maps of twenty-first century forest carbon fluxes, *Nat. Clim. Chang.*, 11, 234-240, 10.1038/s41558-
020-00976-6, 2021.
- He, K., Mi, Z., Coffman, D. M., and Guan, D.: Using a linear regression approach to sequential interindustry model for time-
lagged economic impact analysis, *Struct. Change and Econ. Dyn.*, 62, 399-406,
410 <https://doi.org/10.1016/j.strueco.2022.03.017>, 2022.
- Henders, S., Persson, U. M., and Kastner, T.: Trading forests: land-use change and carbon emissions embodied in production
and exports of forest-risk commodities, *Environ. Res. Lett.*, 10, 125012, 10.1088/1748-9326/10/12/125012, 2015.
- Hoang, N. T. and Kanemoto, K.: Mapping the deforestation footprint of nations reveals growing threat to tropical forests,
Nat. Ecol. Evol., 5, 845-853, 10.1038/s41559-021-01417-z, 2021.
- 415 Hochard, J. and Barbier, E.: Market accessibility and economic growth: Insights from a new dimension of inequality, *World
Dev.*, 97, 279-297, 2017.
- Hong, C., Zhao, H., Qin, Y., Burney, J. A., Pongratz, J., Hartung, K., Liu, Y., Moore, F. C., Jackson, R. B., Zhang, Q., and
Davis, S. J.: Land-use emissions embodied in international trade, *Science*, 376, 597-603, 10.1126/science.abj1572, 2022.
- Hosseiny, B., Zaboli, M., and Homayouni, S.: Forest Change Mapping using Multi-Source Satellite SAR, Optical, and
420 LiDAR Remote Sensing Data, *ISPRS Annals of the Photogrammetry, Remote Sensing and Spatial Information Sciences*,
163-168, 10.5194/isprs-annals-X-4-2024-163-2024,
- Kanemoto, K., Moran, D., and Hertwich, E. G.: Mapping the Carbon Footprint of Nations, *Environ. Sci. Technol.*, 50,
10512-10517, 10.1021/acs.est.6b03227, 2016.
- Lambin, E. F., Gibbs, H. K., Heilmayr, R., Carlson, K. M., Fleck, L. C., Garrett, R. D., le Polain de Waroux, Y., McDermott,
425 C. L., McLaughlin, D., Newton, P., Nolte, C., Pacheco, P., Rausch, L. L., Streck, C., Thorlakson, T., and Walker, N. F.: The
role of supply-chain initiatives in reducing deforestation, *Nat. Clim. Chang.*, 8, 109-116, 10.1038/s41558-017-0061-1, 2018.
- Lenzen, M., Moran, D., Kanemoto, K., and Geschke, A.: Building Eora: a global multi-region input-output database at high
country and sector resolution, *Econ. Syst. Res.*, 25, 20-49, 10.1080/09535314.2013.769938, 2013.
- Lenzen, M., Sun, Y.-Y., Faturay, F., Ting, Y.-P., Geschke, A., and Malik, A.: The carbon footprint of global tourism, *Nat.*
430 *Clim. Chang.*, 8, 522-528, 10.1038/s41558-018-0141-x, 2018.
- Liu, W., Zhang, X., Zhao, T., Wang, J., Li, Z., and Liu, L.: Revealing the proximate drivers behind global tree cover loss
using multisourced remote sensing products during 2000–2020, *For. Ecol. Manage.*, 579, 10.1016/j.foreco.2025.122501,
2025.
- Liu, X., Zhang, J., Zhang, H., Tang, D., Hu, G., and Li, X.: China's Mismatch of Public Awareness and Biodiversity Threats
435 under Economic Trade, *Environ. Sci. Technol.*, 56, 9784-9796, 10.1021/acs.est.2c00844, 2022.
- Meijer, J. R., Huijbregts, M. A. J., Schotten, K. C. G. J., and Schipper, A. M.: Global patterns of current and future road
infrastructure, *Environ. Res. Lett.*, 13, 064006, 10.1088/1748-9326/aabd42, 2018.
- Moran, D., Giljum, S., Kanemoto, K., and Godar, J.: From Satellite to Supply Chain: New Approaches Connect Earth



- Observation to Economic Decisions, *One Earth*, 3, 5-8, 10.1016/j.oneear.2020.06.007, 2020.
- 440 Nelson, A., Weiss, D. J., van Etten, J., Cattaneo, A., McMenemy, T. S., and Koo, J.: A suite of global accessibility indicators, *Sci. Data*, 6, 266, 10.1038/s41597-019-0265-5, 2019.
- Pendrill, F., Persson, U. M., Godar, J., and Kastner, T.: Deforestation displaced: trade in forest-risk commodities and the prospects for a global forest transition, *Environ. Res. Lett.*, 14, 055003, 10.1088/1748-9326/ab0d41, 2019a.
- 445 Pendrill, F., Persson, U. M., Godar, J., Kastner, T., Moran, D., Schmidt, S., and Wood, R.: Agricultural and forestry trade drives large share of tropical deforestation emissions, *Glob. Environ. Change-Human Policy Dimens.*, 56, 1-10, 10.1016/j.gloenvcha.2019.03.002, 2019b.
- Souza Jr, C.: Assessing the scale of rubber deforestation in southeast Asia, *Nature*, 623, 256-257, 10.1038/d41586-023-03153-9, 2023.
- Tang, D., Yao, Y., Li, R., and Li, X.: Consumption-based Carbon Emissions for Deforestation (2001–2020), figshare [dataset], <https://doi.org/10.6084/m9.figshare.28091879.v3>, 2024.
- 450 Verburg, P. H., Ellis, E. C., and Letourneau, A.: A global assessment of market accessibility and market influence for global environmental change studies, *Environ. Res. Lett.*, 6, 034019, 10.1088/1748-9326/6/3/034019, 2011.
- Wang, Y., Hollingsworth, P. M., Zhai, D., West, C. D., Green, J. M. H., Chen, H., Hurni, K., Su, Y., Warren-Thomas, E., Xu, J., and Ahrends, A.: High-resolution maps show that rubber causes substantial deforestation, *Nature*, 623, 340-346, 455 10.1038/s41586-023-06642-z, 2023.
- Weiss, D. J., Nelson, A., Gibson, H. S., Temperley, W., Peedell, S., Lieber, A., Hancher, M., Poyart, E., Belchior, S., Fullman, N., Mappin, B., Dalrymple, U., Rozier, J., Lucas, T. C. D., Howes, R. E., Tusting, L. S., Kang, S. Y., Cameron, E., Bisanzio, D., Battle, K. E., Bhatt, S., and Gething, P. W.: A global map of travel time to cities to assess inequalities in accessibility in 2015, *Nature*, 553, 333-336, 10.1038/nature25181, 2018.
- 460 Wiedmann, T. and Lenzen, M.: Environmental and social footprints of international trade, *Nat. Geosci.*, 11, 314-321, 10.1038/s41561-018-0113-9, 2018.
- Yang, Y., Qu, S., Cai, B., Liang, S., Wang, Z., Wang, J., and Xu, M.: Mapping global carbon footprint in China, *Nat. Commun.*, 11, 2237, 10.1038/s41467-020-15883-9, 2020.